A Cardinal-Direction Quincunx Based Interpolation Technique with Non-Uniform Inter-Plane Weighting for Bayer CFA Demosaicking

Kinyua Wachira and Elijah Mwangi
School of Engineering,
University of Nairobi,
Kenya
Email: kinyua.wachira@students.uonbi.ac.ke

***Abstract*—This paper presents a new weighted interpolation technique to address the Bayer Color Filter Array (CFA) demosaicking problem. The proposed technique provides two contributions that have not been reported in conventional interpolation methods. Firstly, it exploits the quincuncial nature of the green component of the Bayer CFA. The second contribution treats each of the three planes or lattices of the CFA mosaic as distinct and is weighted uniquely. The proposed technique is compared with other interpolation-based demosaicking algorithms and a significant improvement in performance has been noted through experimental results. In addition, to provide objectivity in analysis, three test measures have been used - CPSNR, CIELAB and CIEDE2000.**

Keywords*—*Demosaicking, inter-plane weighting, positive contributors, negative contributors, quincunx.

I. Introduction

The digital still camera has become an ubiquitous feature in human society. It is found either as a stand-alone object or integrated into another device. The process of image capture consists of several stages such as focus and exposure control, white balance adjustment, demosaicking, color transformation, correction [1]. This paper concerns itself with the demosaicking stage.

To produce a color image, there should be three color samples per sampling point; usually red, green and blue [2]. To achieve this, the digital camera has either a three color sensor regime or a single color sensor type that incorporates a technique to establish the unsampled points [3]. The second method is preferred as it reduces the camera's cost and complexity. A Color Filter Array (CFA) is used to perform the discrimination of the incident light from the lens into a one color per pixel sensor. The particular CFA in Figure 1 is the most commonly used and documented; the Bayer CFA, developed in 1976 [4].

The image on camera sensor follows the orientation set by the CFA. A demosaicking algorithm is used to reconstruct each of the constituent color planes from the CFA representation. Due to the popularity of CFA based cameras, the demosaicking problem has been and still is an area of extensive study. Li *et al.* [3] made a recent survey and classified demosaicking algorithms as either motivated in the spatial-domain, the frequency-domain such as in [5] or a hybrid of the two [6]. This paper is biased towards spatial domain based demosaicking techniques

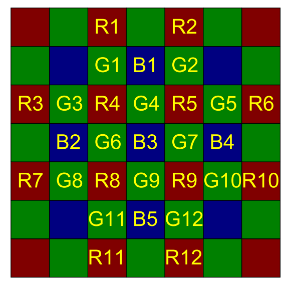

Fig. 1. The Bayer CFA arrangement in a 7-by-7 window

as they produce good, robust results and they are of moderate computational complexity.

In the simplest case, spatial demosaicking can be implemented by Bilinear Interpolation (BI). However, the high correlation between different color planes is not exploited. This results in color abnormalities in the final reconstructed image [7]. The constant hue based interpolation techniques assume that the hue content in an image is roughly constant. This assumption has been exploited for non-green planes in [8]. The main methods here are the Constant Difference Based Interpolation (CDBI) and Constant Ratio Based Interpolation (CRBI) [7].

Edge Directed Interpolation (EDI) introduced by Laroche *et al.* [9] is an adaptive method that uses neighbor information to determine which edge to interpolate along. Hamilton and Adams [10] and Chang *et al.* [11] extend this method by using gradients as correction terms in the red and blue planes. A more recent variant of EDI is Direction Weighted Interpolation (DWI) technique [12]. This method not only collects edge information but each edge is weighted by a gradient-based factor. This method in turn has been extended recently in various ways such as the Malvar-He-Cutler (MHC) algorithm in [13], the Wang method [14] and the Multi-Directional Weighted Interpolation (MDWI) [15].

Our proposed algorithm extends the preliminary section of the MDWI method by offering two novel contributions: an exploitation of the quincunx arrangement of the green plane and non-uniform inter-plane weighting.

The remainder of this paper is divided as follows. Section II explains the two new contributions in detail before the

978-1-4799-1823-2/15/$31.00 ©2015 IEEE

entire algorithm is presented. Section III shows the objective evaluation mechanisms chosen and the rationale behind them. Finally Section IV briefly presents the conclusions that are drawn from experimental results.

II. Proposed Technique

A. Full Exploitation of the Quincunx Arrangement

The proposed technique offers two novel properties to conventional weighted interpolation. The first is exploitation of the full quincunx of the window bounding our pixel of interest. This arrangement is particular to the Bayer CFA and its direct variants.

Figure 2 shows some demosaicking techniques and their quincunx arrangements in the desired pixel's region of interest. Used points are marked in green, unused ones are shown in olive and the desired pixel point is marked in gray. In EDI, DWI and MDWI cases, not all the green pixels in the quincunx arrangement of the bounding window are used. In these methods the window is made large to give a better estimation in the interpolation direction. Size is crucial because a small window gives insufficient points and a large one introduces errors due to distance from the desired pixel. The effect of inaccurate points in a large window can be reduced by forcing them to make a small contribution. However that, in the limit, leads back to the small window problem.

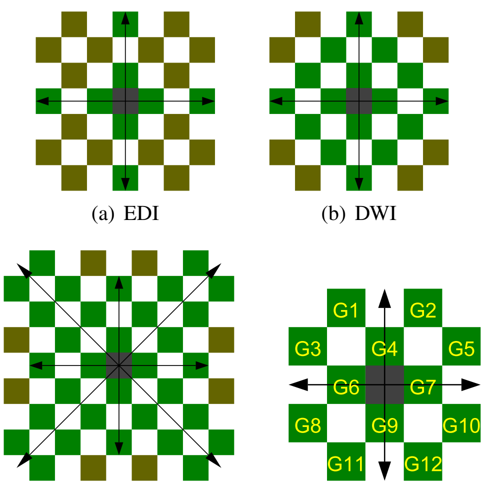

(a) EDI (b) DWI (c) MDWI (d) Proposed

Fig. 2. A comparison of effective pixel usage in the green quincunx plane

The proposed method instead picks all members of the quincunx arrangement in a 5-by-5 bounding window and classifies them in the cardinal directions. In Figure 2(d) pixels G1,G2,G3,G4,G5 contribute to the north direction since they all appear north of the desired pixel. By the same token G2,G5,G7,G10 and G12 are used for the east direction. A measure of quincunx use is given by equation 1. In terms of n_Q, EDI has 0.333; DWI has 0.667; MDWI has 0.8 and the proposed method has a $n_Q = 1$.

$$\eta_Q = (G_{used})/(G_{total}) \tag{1}$$

Conventional weighted techniques have the gradient made up of a sum of positive differences as the pixels chosen already conform to the desired direction. In the proposed technique, a sufficient weighted sum will consist of positive (G_{diff+}) and negative (G_{diff-}) terms. This is because there are some green pixel differences in line with the desired edge while others are in directional opposition to the edge.

$$\bigtriangledown G = \sum_m G_{diff+} + \sum_n G_{diff-} \tag{2}$$

Consider the green pixels in Figure 3(a). There are 7 paths between closest neighbors between the 5 pixels. Paths 1,3,6 and 7 are diagonal. From a 'pseudo-vector' viewpoint shown in Figure 3(b), the overall direction follows a vertical path. Therefore, differences along these paths are taken as positive.

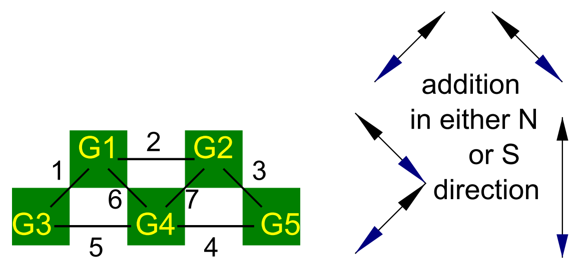

(a) Subset from Figure 2(d) (b) Pseudo-vector addition

Fig. 3. Quincunx paths

Paths 2,4 and 5 are all horizontal. This direction being opposite to the vertical lets us treat the paths as negative contributors. So in equation 2 considering the North direction, $\sum_m G^N_{diff+} = (|G4-G1|+|G4-G2|+|G3-G1|+|G5-G2|)$ and $\sum_n G^N_{diff-} = (|G4-G3|+|G4-G5|+|G1-G2|)$.

To further refine equation 2, two considerations are made. First, the term of path 2 is ignored due to its distance from the desired pixel point. Second, it is undesirable to interpolate across edges [7]. As such the negative contributors are weighted with a factor that is smaller than that used by the positive contributors. For the North direction example:

$$\bigtriangledown G^N = \{c_1 \sum_m G^N_{diff_+}\} - \{c_2 \sum_{n-1} G^N_{diff_-}\} \tag{3}$$

where $c_2 < c_1$. It was determined empirically that $c_1 = 1$ and $c_2 = 0.707$ gave good results.

B. Non-uniform Inter-plane Weighting

A Bayer CFA is a mosaic of 3 separate color planes [4], that are essentially superimposed on one another. If a section of Figure 1 is split plane-wise, Figure 4 is obtained.

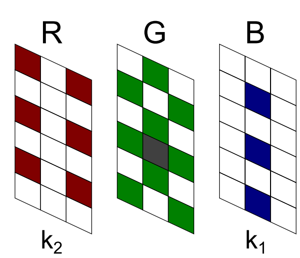

Fig. 4. A Bayer CFA portion split into its constituent planes

Consider the process of determining the pixel point marked gray in Figure 4. The desired information is the green content in a blue pixel point. Conventional interpolation techniques employ the following general equation:

$$\bigtriangledown = \bigtriangledown G + \bigtriangledown B + \bigtriangledown R \tag{4}$$

and $\bigtriangledown X = \sum X_{diff}$ where $X \subset G, B, R$.

From equation 4, it is noted that all planes are treated as equal or $k_1 = k_2 = 1$ in Figure 4. The authors propose that if k_1 and k_2 are taken as variable, there are three possible inter-plane relations. Either $k_1 = k_2 = 1$ or $k_1 = k_2 \neq 1$ or $k_1 \neq k_2 \neq 1$.

In terms of weight priority in Figure 4, intuitively green is first, followed by blue then red. The green plane is where the missing color resides. The blue plane shares the same pixel location as the desired color. The red plane does not contain either the missing color or the pixel point and should contribute the least. The proposed algorithm quantifies this priority by using non-uniform inter-plane weighting where $k_2 < k_1 < 1$. This is a subset of the relation $k_1 \neq k_2 \neq 1$. From empirical testing, it was established that $k_1 = 0.8$ and $k_2 = 0.7$ gave good overall results. This generalizes equation 4 to:

$$\bigtriangledown = \bigtriangledown G + \bigtriangledown B' + \bigtriangledown R' \tag{5}$$

where $\bigtriangledown B' = k_1 \times \bigtriangledown B$ and $\bigtriangledown R' = k_2 \times \bigtriangledown R$.

C. Interpolation of Missing Components in the Green Plane

Consider establishing the green content value at pixel B3 of the Bayer CFA in Figure 1. Initial estimates are first made in the cardinal directions:

$$\begin{aligned} G^N_{B3} &= G4 + \{(k_1 k_2)(B3 - B1)\} \\ G^W_{B3} &= G6 + \{(k_1 k_2)(B3 - B2)\} \\ G^E_{B3} &= G7 + \{(k_1 k_2)(B3 - B4)\} \\ G^S_{B3} &= G9 + \{(k_1 k_2)(B3 - B5)\} \end{aligned} \tag{6}$$

Inter-plane weighting is used as the estimates will in the final analysis will be weighted by both red and blue planes. The gradients in each cardinal directions are then established following equation 4. Consider the West direction:

$$\bigtriangledown^W_{B3} = \bigtriangledown G^W_{B3} + \bigtriangledown B^W_{B3} + \bigtriangledown R^W_{B3} \tag{7}$$

The green contribution of the gradient will use the quincunx arrangement while the red and blue contributions of the gradient will use the inter-plane weighting concept.

$$\bigtriangledown G^W_{B3} = c_1 \sum G^W_{B3+} - c_2 \sum G^W_{B3-} \tag{8}$$

where $\sum G^W_{B3+} = (|G6 - G3| + |G6 - G8| + |G1 - G3| + |G11 - G8|)$ and $\sum G^W_{B3-} = (|G6 - G1| + |G6 - G11|)$.

$$\bigtriangledown B^W_{B3} = k_1(|B3 - B2|) \tag{9}$$

$$\bigtriangledown R^W_{B3} = k_2(|R4 - R3| + |R8 - R7|) \tag{10}$$

$\bigtriangledown^N_{B3}$, $\bigtriangledown^E_{B3}$ and $\bigtriangledown^S_{B3}$ are found in a similar manner. Once all the gradients are established, the weights are determined as:

$$w^k_{B3} = \frac{1}{\bigtriangledown^k_{B3}} \tag{11}$$

where $k = \{N, W, E, S\}$. Finally, the value of the green content in pixel B3 is given as:

$$G_{B3} = \frac{\sum_{k=\{N,W,E,S\}} [w^k_{B3} G^k_{B3}]}{\sum_{k=\{N,W,E,S\}} w^k_{B3}} \tag{12}$$

When establishing the green content in a red pixel point, the above relations from equation 6 to 12 should hold. Only the positions of the red and blue pixels are interchanged.

D. Interpolation of Missing Components in the Red/Blue Planes

When looking for missing components in these planes, two possibilities arise. The component resides in the opposing plane, that is, blue in a red pixel point or red in a blue pixel point. The second is that it is in a green pixel point. Both possibilities are illustrated in Figure 5.

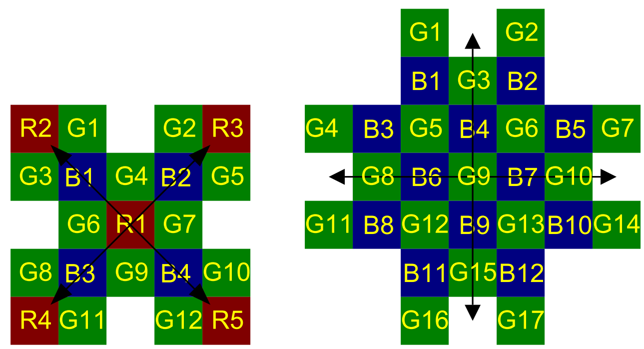

(a) The Opposing Red Plane (b) The Green Plane

Fig. 5. Establishing the missing blue content in different color pixel points

1) Opposing Plane Interpolation: Let us consider the case of finding the missing content in an opposing plane. Using the example of Figure 5(a), assume the blue content in the red pixel R1 needs to be found. As the green plane has already been fully populated, a difference based interpolation solution similar to that seen in [15] is used. The initial difference based estimates taken in the NW, NE, SE and SW directions are then found as:

$$\begin{aligned} \beta^{NW}_{BG} &= B1 - G_{B1}, \beta^{NE}_{BG} = B2 - G_{B2} \\ \beta^{SE}_{BG} &= B4 - G_{B4}, \beta^{SW}_{BG} = B3 - G_{B3} \end{aligned} \tag{13}$$

Next the gradients are established and in each direction, there will be three type of contributors. The green pixels that lie exactly in the desired direction, the green pixels that are outliers of the desired direction and third the blue pixels that lie in the desired direction. They will follow that order of precedence:

$$\phi_{dir} = \sum G_{dir} + \sum G_{out} + \sum B_{dir} \tag{14}$$

To provide appropriate weighting to implicitly put the above priority into our weights, k_1 and k_2 are used. This can be envisioned intuitively as if the three contributors themselves are different pseudo-planes in this difference based relation of equation 13. For the North West direction, from equation 14, $\sum G^{NW}_{dir} = |G_{R1} - G_{B1}| + |G_{B1} - G_{R2}|$,

$\sum G_{out}^{NW} = |G4 - G1| + |G6 - G3|$ and $\sum B_{dir}^{NW} = |B4 - B1|$. The same technique is used to establish ϕ_{NE}, ϕ_{SE} and ϕ_{SW}.

The weights are then determined in a manner similar to equation 11:

$$\Phi_{k=\{NW,NE,SE,SW\}} = \frac{1}{\phi_k} \tag{15}$$

The value of the blue content in the red pixel point is then determined as follows:

$$B_{R1} = G_{R1} + \frac{\sum_{k=\{NW,NE,SE,SW\}}[\Phi_k \beta_{BG}^k]}{\sum_{k=\{NW,NE,SE,SW\}} \Phi_k} \tag{16}$$

2) Green Plane Interpolation: Let us consider interpolating the blue content G9 in Figure 5(b). The blue plane is now quincunx in nature. This allows the use of closer proximity pixels for the interpolation process. The initial estimates are determined as in equation 6. An example is given for the North direction in equation 17,

$$B_{G9}^N = B4 + k1|G9 - G3| \tag{17}$$

It should be noted that only k_1 is used in equation 17. This is because only two planes are under consideration. The gradients here are obtained in a similar manner as when the green plane was interpolated.

$$\triangledown = \triangledown B + \triangledown G' \tag{18}$$

where $\triangledown G' = k_1 \times \triangledown G$.

For the North direction example, the blue and green gradient terms are established by:

$$\triangledown B_{G9}^N = |B6 - B1| + |B7 - B2| + |B4 - B1| + |B4 - B2| \tag{19}$$

$$\triangledown G_{G9}'^N = k_1(|G5 - G1| + |G6 - G2| + |G9 - G3|) \tag{20}$$

The above two equation combined result in the directional form of equation 18

$$\triangledown_{G9}^N = \triangledown B_{G9}^N + \triangledown G_{G9}'^N \tag{21}$$

The other gradients $\triangledown_{G9}^W$,$\triangledown_{G9}^E$ and $\triangledown_{G9}^S$ are found. The weights w_{G9}^N,w_{G9}^E w_{G9}^S and w_{G9}^W are obtained and finally:

$$B_{G9} = \frac{\sum_{k=\{N,W,E,S\}}[w_{G9}^k B_{G9}^k]}{\sum_{k=\{N,W,E,S\}} w_{G9}^k} \tag{22}$$

The treatment presented here is for the missing component in the blue plane. The red plane situation is treated in the exact same manner.

III. Experimental Results

A. Choice of Image Set

The Kodak image set [16] was used. This is because most of the comparison techniques used to gauge the proposed method used that set.

B. Evaluation Measures Used

Three objective measures were used. These are the color peak signal-to-noise ratio (CPSNR) and two of the International Commission on Illumination (CIE) measures: CIELAB ($\triangle E_{ab}^*$) and CIEDE2000 ($\triangle E_{00}$). CPSNR is defined in the RGB color space and is an extension of conventional PSNR. It is an absolute measure that does not take into consideration the human visual system that follows a hue, saturation and lightness (HSL) based color space [1]. The larger the value of CPSNR the better the reconstructed image is.

$$CPSNR = 10log_{10}(\frac{255^2}{CMSE}) \tag{23}$$

$$CMSE = \frac{\sum_1^r \sum_1^c \sum_{k=R,G,B}(A_{i,j,k} - \tilde{A}_{i,j,k})}{3rc} \tag{24}$$

The second set of metrics are defined in a HSL-based color space by CIE called L*a*b* [17]. L* is luminosity information and a* and b* provide chromacity information. CIELAB was the initial difference equation. CIEDE2000 offers some improvements to measure differences in the L*a*b* space [18], [19]. The CIELAB difference equation between two pixel points is given by equation 25. The CIEDE2000 color difference formula used between two points is modestly given in equation 26. However a full representation is provided in [19].

$$\triangle E_{ab}^{*12} = \left[(L_1^* - L_2^*)^2 + (a_1^* - a_2^*)^2 + (b_1^* - b_2^*)^2\right]^{1/2} \tag{25}$$

$$\triangle E_{00}^{12} = \triangle E_{00}(L_1^*, a_1^*, b_1^*, L_2^*, a_2^*, b_2^*) \tag{26}$$

To apply equations 25 and 26, all pixel point differences must be summed over the entire image region. The smaller the value of the CIELAB and CIEDE2000 differences, the closer the reconstructed image is to the original.

C. Performance Results

The performance of the proposed algorithm was compared with nine other interpolation based demosaicking techniques. These are BI, CDBI and CRBI [7]; EDI [9]; HA [10]; Chang [11]; MHC [13]; the Wang algorithm [14] and MDWI [15]. To validate the proposed algorithm, the authors conducted simulations using MATLAB R2013a on an Intel(R) Core(TM)2 Duo CPU E7500 @2.93 GHz processor. It should be noted that no post-processing was implemented in any of the algorithms. This was because the authors wanted to determine the performance prior to post-processing. Also no formal algorithm complexity analysis was performed. Complexity tends to increase with the number of descriptors. In general BI, CDBI and CRBI have a low algorithmic complexity. EDI, HA, Chang and MHC are moderate while Wang and MDWI have the highest complexity of the chosen algorithms. The proposed algorithm is between a moderate and a high complexity.

First, the complete Kodak image set was applied to each of the demosaicking algorithms in turn. At each stage, the measures of CPSNR, CIELAB and CIEDE2000 were noted. An arithmetic mean (denoted M_A) of the set was done for each algorithm. All the results were then tabulated in Tables I to III with the proposed algorithm results in the Prop. column.

TABLE I. CPSNR RESULTS FOR DIFFERENT DEMOSAICKING TECHNIQUES ON THE KODAK IMAGE SET (IN DB)

Image	BI	CDBI	CRBI	Chang	EDI	HA	MHC	Wang	MDWI	Prop.
01	26.37	29.15	28.94	24.30	29.57	32.61	32.04	32.04	32.87	33.78
02	33.48	36.06	33.72	15.95	35.95	38.34	38.05	38.12	38.57	39.17
03	34.68	36.95	36.43	21.17	37.13	39.94	39.39	38.38	39.98	40.05
04	33.88	36.41	33.60	21.18	35.97	38.83	39.15	37.39	38.75	38.88
05	26.82	29.58	28.97	25.02	29.95	32.63	33.22	31.54	34.03	33.22
06	28.03	30.55	30.43	25.61	30.49	33.90	33.28	33.16	34.12	34.71
07	33.63	36.39	35.89	24.55	37.03	39.92	39.36	39.13	40.14	39.60
08	23.82	26.69	26.61	24.83	28.26	28.83	29.07	30.63	31.61	31.85
09	32.64	35.31	35.18	27.80	36.21	38.57	38.09	38.79	39.30	39.34
10	32.63	35.21	35.02	29.37	35.70	38.10	38.61	36.24	39.15	39.11
11	29.41	32.00	31.64	27.08	32.21	34.86	34.79	34.65	35.66	36.28
12	33.57	36.13	35.96	26.63	36.55	39.80	38.78	39.32	39.69	40.38
13	24.05	26.47	26.36	24.86	25.84	28.60	29.49	27.73	29.27	30.28
14	29.53	32.05	31.39	21.04	32.05	34.40	34.27	33.59	35.19	34.68
15	32.49	35.06	33.24	20.72	35.00	37.12	37.39	36.44	37.66	37.81
16	31.51	33.99	33.88	29.53	34.04	37.93	36.62	36.89	37.39	38.33
17	32.27	34.81	34.60	29.72	34.71	36.96	37.69	36.50	37.77	38.06
18	28.14	30.68	30.36	24.03	30.07	32.61	33.48	31.88	33.22	33.59
19	28.24	31.14	30.89	24.48	33.19	33.86	33.66	35.68	36.06	36.27
20	31.83	34.29	34.08	11.85	34.84	37.20	36.99	36.54	37.03	38.31
21	28.72	31.33	31.15	25.25	31.22	34.47	34.14	33.55	34.80	35.24
22	30.70	33.21	32.96	23.99	33.17	35.06	35.32	34.77	35.92	35.90
23	35.27	38.24	37.39	19.35	38.23	40.29	40.95	39.67	40.91	39.84
24	26.87	29.33	29.21	16.98	28.76	30.73	31.68	29.99	31.44	32.00
M_A	30.36	32.96	32.41	23.55	33.17	35.65	35.65	35.11	36.27	**36.53**

TABLE II. CIELAB $\triangle E^*_{ab}$ RESULTS FOR DIFFERENT DEMOSAICKING TECHNIQUES ON THE KODAK IMAGE SET

Image	BI	CDBI	CRBI	Chang	EDI	HA	MHC	Wang	MDWI	Prop.
01	9.159	7.173	7.390	10.396	6.305	4.597	5.054	4.910	4.312	4.110
02	3.783	3.014	4.222	26.908	2.735	2.268	2.419	2.451	2.147	2.203
03	3.050	2.537	2.732	9.664	2.189	1.688	1.791	2.014	1.665	1.660
04	3.871	3.079	4.068	13.739	2.956	2.348	2.301	2.721	2.209	2.223
05	8.276	6.576	7.040	8.833	5.790	4.125	4.206	4.700	3.806	3.916
06	6.836	5.501	5.557	7.634	4.866	3.339	3.875	3.736	3.418	3.241
07	3.421	2.806	2.987	7.876	2.282	1.821	1.996	2.061	1.739	1.900
08	11.120	8.699	8.818	9.490	6.346	5.708	6.184	4.998	4.717	4.600
09	3.802	3.131	3.245	4.395	2.640	2.139	2.242	2.267	2.030	2.015
10	3.749	3.101	3.219	4.414	2.660	2.083	2.161	2.356	1.995	1.984
11	5.713	4.570	4.790	6.591	4.054	2.981	3.293	3.237	2.897	2.745
12	3.477	2.843	2.961	6.696	2.439	1.861	2.062	2.068	1.837	1.803
13	11.693	9.327	9.422	10.560	9.678	6.740	6.587	7.681	6.575	5.731
14	6.254	4.968	5.347	9.666	4.592	3.338	3.517	3.830	3.202	3.234
15	4.000	3.236	3.965	9.814	2.935	2.415	2.405	2.681	2.215	2.282
16	4.837	3.923	3.986	5.334	3.452	2.392	2.826	2.736	2.533	2.383
17	4.009	3.268	3.418	4.699	2.962	2.270	2.334	2.542	2.209	2.172
18	6.761	5.430	5.627	8.985	5.512	4.039	3.823	4.544	3.789	3.683
19	6.131	4.891	5.066	8.719	3.852	3.393	3.525	3.246	2.897	2.816
20	3.779	3.120	3.211	20.594	2.715	2.170	2.271	2.368	2.101	1.973
21	6.053	4.868	4.995	8.486	4.582	3.328	3.489	3.759	3.240	3.061
22	5.033	4.133	4.270	9.049	4.010	3.111	3.045	3.498	2.935	2.900
23	2.582	2.176	2.415	11.135	1.976	1.705	1.621	1.868	1.597	1.642
24	6.824	5.445	5.558	11.140	5.073	3.801	3.783	4.253	3.564	3.418
M_A	5.592	4.492	4.763	9.784	4.025	3.069	3.200	3.355	2.901	**2.821**

TABLE III. CIEDE2000 $\triangle E_{00}$ RESULTS FOR DIFFERENT DEMOSAICKING TECHNIQUES ON THE KODAK IMAGE SET

Image	BI	CDBI	CRBI	Chang	EDI	HA	MHC	Wang	MDWI	Prop.
01	3.577	2.820	2.858	3.180	2.441	1.728	1.795	1.846	1.686	1.600
02	1.579	1.260	1.728	8.127	1.130	0.923	0.943	0.993	0.885	0.896
03	1.175	0.981	1.029	2.391	0.831	0.630	0.643	0.745	0.628	0.628
04	1.638	1.301	1.755	4.219	1.246	0.969	0.900	1.121	0.921	0.915
05	3.801	3.044	3.217	2.870	2.666	1.797	1.725	2.083	1.729	1.699
06	2.522	2.024	2.002	1.959	1.776	1.189	1.294	1.340	1.254	1.188
07	1.390	1.159	1.188	1.971	0.912	0.696	0.755	0.787	0.675	0.734
08	4.335	3.402	3.422	2.946	2.480	2.152	2.216	1.918	1.860	1.785
09	1.424	1.171	1.187	1.229	0.954	0.764	0.771	0.796	0.727	0.727
10	1.438	1.193	1.218	1.232	1.002	0.764	0.765	0.861	0.740	0.739
11	2.399	1.930	1.975	1.993	1.705	1.217	1.264	1.324	1.210	1.121
12	1.156	0.938	0.956	1.499	0.793	0.596	0.627	0.664	0.598	0.591
13	4.724	3.791	3.769	3.154	3.926	2.645	2.424	3.069	2.704	2.312
14	2.690	2.158	2.278	2.635	1.980	1.399	1.380	1.608	1.370	1.346
15	1.707	1.382	1.722	3.118	1.265	1.009	0.938	1.126	0.945	0.947
16	2.106	1.726	1.715	1.612	1.488	1.000	1.128	1.141	1.089	1.001
17	1.740	1.435	1.464	1.453	1.294	0.960	0.934	1.072	0.950	0.909
18	3.049	2.493	2.523	2.697	2.522	1.767	1.588	2.013	1.710	1.621
19	2.371	1.914	1.936	2.309	1.586	1.307	1.230	1.303	1.166	1.095
20	1.520	1.262	1.264	5.989	1.100	0.831	0.818	0.919	0.819	0.750
21	2.482	2.007	2.019	2.325	1.879	1.315	1.304	1.496	1.314	1.221
22	1.928	1.595	1.616	2.298	1.541	1.144	1.076	1.302	1.102	1.080
23	1.007	0.850	0.935	2.738	0.748	0.636	0.585	0.694	0.593	0.613
24	2.615	2.102	2.116	3.304	1.919	1.394	1.349	1.572	1.335	1.289
M_A	2.266	1.831	1.912	2.802	1.633	1.201	1.185	1.325	1.167	**1.117**

Table I highlights the CPSNR performance. Table II and III show the CIELAB and CIEDE2000 values providing a measure for human vision. A marked improvement over established methods is noted as the proposed algorithm had the highest mean CPSNR and the lowest mean CIELAB and CIEDE2000 values. This is an objective indication of image acuity.

IV. CONCLUSION

A new interpolation based demosaicking technique was proposed with two new contributions. To provide objectivity in analysis, three performance metrics: CPSNR, CIELAB and CIEDE2000 were used. Through mean value information, the proposed technique showed a marked improvement over the selected interpolation-based demosaicking techniques. Furthermore, the two contributions offered by the proposed technique are deemed as transferable meaning established techniques can also incorporate them to yield better results.

REFERENCES

[1] R. Ramanath, W. E. Snyder, Y. Yoo, and M. S. Drew, "Color image processing pipeline," *IEEE Signal Process. Mag.*, vol. 22, pp. 34–43, Jan. 2005.

[2] M. Vrhel, E. Saber, and H. J. Trussel, "Color image generation and display technologies," *IEEE Signal Process. Mag.*, vol. 22, pp. 23–33, Jan. 2005.

[3] X. Li, B. K. Gunturk, and L. Zhang, "Image demosaicking: A systematic survey," in *Proc. SPIE 6822, Visual Communications and Image Processing 2008, SPIE-IS&T Electronic Imaging*, San Jose, CA, Jan. 2008.

[4] B. E. Bayer, "Color imaging array," U.S. Patent 3 971 065, Jul. 20, 1976.

[5] D. Alleysson, S. Süsstrunk, and J. Hérault, "Linear demosaicing inspired by the human visual system," *IEEE Trans. Image Process.*, vol. 14, no. 4, pp. 1–12, Apr. 2005.

[6] K. Hirakawa and P. J. Wolfe, "Spatio-Spectral color filter array design for optimal image recovery," *IEEE Trans. Image Process.*, vol. 17, no. 10, pp. 1876–1890, Oct. 2008.

[7] B. K. Gunturk, J. Glotzbach, Y. Altunbasak, R. W. Schafer, and R. M. Mersereau, "Demosaicking: Color filter array interpolation," *IEEE Signal Process. Mag.*, vol. 22, pp. 44–54, Jan. 2005.

[8] W. T. Freeman, "Median filter for reconstructing missing color samples," U.S. Patent 4 724 395, Feb. 9, 1988.

[9] C. A. Laroche and M. A. Prescott, "Apparatus and method for adaptively interpolating a full color image utilizing chrominance gradients," U.S. Patent 5 373 322, Dec. 13, 1994.

[10] J. E. Adams and J. F. Hamilton, "Adaptive color plan interpolation in single sensor color electronic camera," U.S. Patent 5 506 619, Apr. 9, 1996.

[11] E. Chang, S. Cheung, and D. Pan, "Color filter array recovery using a threshold-based variable number of gradients," in *Proc. SPIE 3650, IS&T/SPIE Conference on Sensors, Cameras and Applications for Digital Photography*, San Jose, CA, Jan. 1999.

[12] W. Lu and Y.-P. Tan, "Color filter array demosaicking: New method and performance measures," *IEEE Trans. Image Process.*, vol. 12, no. 10, pp. 1194–1210, Oct. 2003.

[13] P. Getreuer, "Malvar-He-Cutler linear image demosaicking," *Image Processing On Line (IPOL)*, vol. 1, Aug. 2011.

[14] W. Jin, "Improved color interpolation method based on bayer image," in *Proc. SPIE 8420, 6th International Symposium on Advanced Optical Manufacturing and Testing Technologies*, 2012.

[15] X. Chen, G. Jeon, J. Jeong, and L. He, "Multi-directional weighted interpolation and refinement method for bayer pattern cfa demosaicking," *IEEE Trans. Circuits Syst. Video Technol.*, submitted for publication in 2014.

[16] (2014). [Online]. Available: http://r0k.us/graphics/kodak/

[17] *ISO 11664-4:2008(E)/CIE S 014-4/E:2007 Joint ISO/CIE Standard: Colorimetry Part 4: CIE 1976 L*a*b* Colour Space*, ISO/CIE Std., 2008.

[18] *ISO/CIE 11664-6:2014(E): Colorimetry - Part 6: CIEDE2000 Colour-Difference Formula*, ISO/CIE Std., 2008.

[19] G. Sharma, W. Wu, and E. N. Dalal, "The CIEDE2000 Color-Difference Formula: Implementation notes, supplementary test data, and mathematical observations," *Color Research and Application*, vol. 30, no. 1, pp. 21–30, Feb. 2005.